

ORIGINAL ARTICLE

Iran J Allergy Asthma Immunol

In press.

Zinc Oxide Nanoparticles Modulate PBMC Cytokines and Trigger Cytotoxicity, Apoptosis, and Anti-angiogenic Effects in HeLa Cells in Co-culture

Milad Karimi Aftab¹, Reza Falak^{2,3}, Ramezan Ali Taheri⁴, Zeinab Baghernejadan³, and Mahdi Fasihi-Ramandi¹

¹ Molecular Biology Research Center, Biomedicine Technologies Institute, Baqiyatallah University of Medical Sciences, Tehran, Iran

² Breast Cancer Research Center, Iran University of Medical Sciences, Tehran, Iran

³ Department of Immunology, School of Medicine, Iran University of Medical Sciences, Tehran, Iran

⁴ Nanobiotechnology Research Center, New Health Technologies Institute, Baqiyatallah University of Medical Sciences, Tehran, Iran

Received: 13 December 2025; Received in revised form: 7 January 2026; Accepted: 1 February 2026

ABSTRACT

Cervical cancer is the fourth most prevalent malignancy among women globally. Zinc oxide nanoparticles (ZnO-NPs) possess significant potential in cancer therapy due to their unique physicochemical properties, biocompatibility, and apoptosis-inducing abilities. While ZnO-NPs have been examined in HeLa cells and peripheral blood mononuclear cells (PBMCs) individually, their immunological and angiogenesis-related effects in immune-tumor co-culture systems was insufficiently investigated. This study assessed the apoptotic, anti-angiogenic, and cytokine-modulating effects of ZnO-NPs in a HeLa/PBMC co-culture model.

HeLa cells were co-cultured with PBMCs and treated with ZnO-NPs under different groups. Cytotoxicity was evaluated using MTT assay, apoptosis was analyzed by flow cytometry, and gene expression levels were measured using real-time PCR.

ZnO-NPs significantly reduced HeLa cells viability with a half maximal inhibitory concentration (IC₅₀) of 7 µg/mL, while PBMCs showed more resistance (IC₅₀=40 µg/mL). In the HeLa/PBMC/ZnO co-culture group, gene expression analysis in PBMCs revealed significant upregulation of *IL1B*, *TNF*, *IFNG*, and *TGFβ1* compared with the HeLa/PBMC group, while *IL2* and *IL4* expression levels showed no significant changes. *VEGFA* expression in HeLa cells was reduced in all treated groups, with the greatest decrease in the HeLa/PBMC/ZnO group. Co-culture with PBMCs and ZnO-NP treatment significantly promoted apoptosis in HeLa cells.

In conclusion, ZnO-NPs induce cytotoxic and anti-angiogenic effects on HeLa cells, particularly within a PBMC co-culture setting, highlighting the contribution of immune-tumor interactions to ZnO-NP-mediated anti-cancer responses; however, more investigations at the protein and functional levels are necessary to validate these effects.

Keywords: Cervical cancer; Co-culture technique; HeLa cells; Nanoparticles; Zinc oxide

Corresponding Author: Mahdi Fasihi-Ramandi, PhD;
Molecular Biology Research Center, Biomedicine Technologies
Institute, Baqiyatallah University of Medical Sciences, Postal code:

1435915381, Tehran, Iran. Tel: (+98 21) 8755 4328, Email
fasihi.m@gmail.com

INTRODUCTION

Cervical cancer, the fourth most prevalent disease diagnosed in women globally, is one of the main causes of cancer-related mortality among women.¹ Over the past decade, there have been major developments in the diagnosis and treatment of cervical cancer. The overall survival has significantly improved as a result of therapeutic advancements, and researchers are attempting to create novel medications to treat cervical cancer. For advanced or metastatic cervical cancer, pembrolizumab, a programmed cell death protein-1 (PD-1)-targeting immunotherapeutic agent, has shown the highest efficacy among current options.² Overall and progression-free survival rates increase when bevacizumab, an anti-vascular endothelial growth factor (VEGF) drug, or chemotherapy is added; nevertheless, these combination treatments still have drawbacks, such as adverse side effects and partial tumor regression.³

Nanoparticles (NPs) have attracted the attention of scientists in recent years because of their high efficacy and safety.⁴ In recent decades, nanotechnology-based therapeutic and diagnostic techniques have shown tremendous promise in improving cancer therapy.⁵ Several types of inorganic metal oxides, such as titanium dioxide (TiO₂), copper (II) oxide (CuO), and zinc oxide nanoparticles (ZnO-NPs), have been developed and are being actively investigated for biomedical applications. Among these, ZnO-NPs have garnered significant attention due to their affordability, ease of synthesis, and unique physicochemical properties. Their small size allows for efficient cellular uptake and bioavailability; making them a favorable option for biomedical use.⁶ Regardless of the synthesis method employed, all types of ZnO-NPs have proved to be efficient in cancer management through mechanisms such as tumor cell apoptosis, anti-angiogenic effects, and targeted drug release.^{7,8}

In addition to their application in the treatment of cancer, ZnO-NPs offer a wide range of other medicinal uses, including antimicrobial, anti-diabetic, anti-inflammatory, anti-aging properties, and also in wound healing and bioimaging studies.^{9,10}

Although numerous studies have examined the effects of ZnO-NPs on individual HeLa cells and peripheral blood mononuclear cells (PBMCs), their impact in immune-tumor co-culture systems were poorly understood. As most previous studies have relied

on monoculture models, they provide limited insight into immune-tumor interactions within the tumor microenvironment (TME). A co-culture model, like HeLa cells with PBMCs, more closely resembles TME, since it includes immune components that may secrete cytokines and communicate with one another across cells, both of which affect tumor behavior and treatment response.¹¹ To address this limitation, the present study employed a HeLa/PBMC co-culture model to investigate the immunomodulatory, cytotoxic, and anti-angiogenic effects of ZnO-NPs in a more physiologically relevant context. Moreover, inclusion of PBMCs provide an immunological environment that enables the assessment of immune-tumor interactions, thereby enhancing the translational relevance of the model compared with monoculture systems. In cervical cancer, effective immune surveillance relies on coordinated interactions between immune cells and tumor cells, and disruption of these interactions can contribute to tumor progression and immune escape.

Cytokines, including *interleukin 1 beta (IL1B)*, *interleukin 2 (IL2)*, *interleukin 4 (IL4)*, *tumor necrosis factor (TNF)*, *transforming growth factor beta 1 (TGFB1)*, and *interferon gamma (IFNG)*, regulate the intricate interactions within TME, influencing immune cell activation, differentiation, and effector activities.¹² Pro-inflammatory cytokines such as *IL1B*, *TNF*, and *IFNG* enhance anti-tumor immunity by increasing cytotoxic responses, whereas *IL4* and *TGFB1* promote immunosuppressive pathways that facilitate tumor immune evasion.¹³ Furthermore, *VEGFA*-mediated angiogenesis stimulates tumor progression and modifies immune cell infiltration.¹⁴ Investigating cytokine and *VEGFA* expression patterns in PBMCs co-cultured with HeLa cells treated with ZnO-NPs helps the identification of immunomodulatory mechanisms that mediate nanoparticle-induced anti-tumor impacts.

The aim of this study was to investigate the immunomodulatory, cytotoxic, apoptotic, and anti-angiogenic effects of ZnO-NPs on HeLa cells within a PBMC co-culture model, in order to better mimic immune-tumor interactions in TME.

MATERIALS AND METHODS

Cell Culture

HeLa cells were purchased from the National Center for Genetic and Biological Resources of Iran (IRBS).

The cells were cultured in Dulbecco's Modified Eagle Medium (DMEM) (Gibco, USA) supplemented with 10% fetal bovine serum (FBS) (Anacell, Iran) and antibiotics, including 100 U/mL penicillin (Gibco, USA), and 100 µg/mL streptomycin (Gibco, USA) and incubated under optimal conditions in a humidified incubator at 37°C with 5% CO₂. All treatments and experiments were performed in duplicate.

Isolation of PBMCs

For the isolation of PBMCs, peripheral blood samples were collected from three healthy donors in tubes containing EDTA anticoagulant after providing written informed consent. The blood samples were diluted 1:1 with phosphate-buffered saline (PBS) and overlaid on Ficoll-Paque with density gradient 1.071 (Pars Azma Teb, IRAN) and mononuclear cells were separated by 20 minutes centrifugation at 400 g. The collected PBMCs were resuspended in RPMI 1640 medium (Gibco, USA) supplemented with 10% FBS for subsequent experiments.

Characterization of ZnO-NPs

The ZnO-NPs used in this study were purchased from US Research Nanomaterials, Inc., Houston, US. The particle size distribution of the ZnO-NPs was determined using DLS (Malvern Zetasizer, UK) and Zetasizer Ver. 6.01 software. The NPs were dispersed in deionized water (dispersant refractive index: 1.33), and measurements were performed at 25.0°C with a viscosity of 0.8872 cP. The sample was prepared using a low-volume disposable sizing cuvette and analyzed under optimized settings.

The morphology and composition of the NPs were examined using a field emission scanning electron microscope (FE-SEM). Furthermore, to assess the elemental types and their distribution within the ZnO-NPs structure, an energy dispersive spectrometer (EDS) system (S-4100, Hitachi, Japan) fitted with the FE-SEM was employed.

Cytotoxicity Assay

To evaluate the cytotoxic effects of ZnO-NPs on HeLa cells and determine their half maximal inhibitory concentration (IC₅₀), MTT assay was employed. HeLa cells were cultured and passaged to acclimate to the culture conditions. Subsequently, 10,000 cells were seeded into each well of a 96-well plate. After overnight incubation, the cells were treated with serial concentrations of ZnO in duplicate manner and

incubated for 24 hours. After removing the supernatant, 100 µL of fresh culture medium containing 0.5 mg/mL MTT (Kiagene, Iran) solution was added to each well, and plates were incubated for three hours at 37°C in a CO₂ incubator.

After carefully removing the supernatant, the formazan crystals were dissolved by adding 100 µL of dimethyl sulfoxide (DMSO) (Kiagene, Iran) to each well. After 10 minutes of incubation, the absorbance was measured at 570 nm using an ELISA reader. The same procedure was conducted to evaluate the effects of ZnO-NPs on PBMCs.

For subsequent gene expression analysis, the IC₅₀ concentration of ZnO-NPs was used, with a seeding density of 200,000 cells per well. Based on the cytotoxicity results, a working concentration of ZnO-NPs was selected for subsequent experiments. Specifically, the IC₅₀ value determined for HeLa cells (7 µg/mL) was used, as PBMCs exhibited a substantially higher IC₅₀ value (40 µg/mL), indicating that this concentration can induce cytotoxic effects in HeLa cells while having minimal impact on PBMC viability.

Co-culture of HeLa Cells with PBMCs

HeLa cells were divided into four experimental groups: HeLa cells co-cultured with PBMCs (HeLa/PBMC), HeLa cells treated with ZnO-NPs (HeLa/ZnO), HeLa cells co-cultured with PBMCs and treated with ZnO-NPs (HeLa/PBMC/ZnO), and untreated control groups (Ctrl).

For cytokine gene expression analyses, untreated PBMCs cultured alone and served as the Ctrl group. For *VEGFA* expression and apoptosis assays, the Ctrl consisted of untreated HeLa cells cultured alone, without PBMCs or ZnO-NPs.

HeLa cells were treated with ZnO-NPs in co-culture with PBMCs and compared to the untreated control for 24 hours. Thereafter, the PBMCs were collected for RNA extraction and gene expression analysis. For co-culture experiments, HeLa cells were seeded in 6-well plates at a density of 2×10^5 cells per well. Subsequently, PBMCs were added at a density of 2×10^6 cells per well, resulting in a HeLa-to-PBMC ratio of 1:10. The co-cultures were then maintained under standard culture conditions for subsequent treatments and analyses.

Total RNA Isolation and Quantitative Real-time PCR Analysis

First of all, total RNA was extracted from both

PBMCs and HeLa cells using the TRIzol method. Briefly, 300 μ l of chloroform (Merck, Germany) was added to each sample containing TRIzol (Thermo Fisher Scientific, USA), and the mixture was centrifuged at 14,000 rpm. After transferring the aqueous phase to a new vial and adding 500 μ l of isopropanol (Merck, Germany), the samples were incubated on ice for 20 min and centrifuged again. The isopropanol was discarded, and 1 ml of 75% ethanol (Merck, Germany) was added to the pellet, followed by another round of centrifugation. Finally, the RNA pellet was air-dried and resuspended in nuclease-free water at 55°C for 5 min. RNA quality and concentration were evaluated using a NanoDrop spectrophotometer, and samples were stored at -70°C.

Subsequently, cDNA synthesis was performed using the Easy cDNA Synthesis Kit (PARSTOUS, Mashhad, Iran) according to the manufacturer's protocol.

To evaluate gene expression levels of *IL1B*, *IL2*, *IL4*, *TNF*, *TGFB1*, *IFNG*, and *VEGFA* in PBMCs, the quantitative PCR (qPCR) method was carried out using qPCRBIO SyGreen® Mix (PCR Biosystems Inc., Pennsylvania, US). Supplementary Table 1 details the features of the primers (Sinaclone, Tehran, Iran) used in this study. Briefly, to perform qPCR, a reaction mixture (20 μ l) containing approximately 1 μ l of cDNA template was prepared. The temperature conditions were optimized based on the specific annealing temperature of each primer set. All reactions were performed by the Rotor-Gene Q thermal cycler (Qiagen, Germany) in duplicate. The housekeeping gene, *actin beta* (*ACTB*), was used as an internal control, and data were analyzed using the $2^{-\Delta\Delta Ct}$ method.

Apoptosis

Apoptosis in HeLa cells was evaluated using the Annexin V-FITC/PI staining method with the FITC Annexin V Apoptosis Detection Kit (BioLegend, USA), following the manufacturer's protocol. HeLa cells were subjected to three experimental conditions: HeLa/PBMC, HeLa/PBMC/ZnO, and HeLa/ZnO. The procedure involved co-culturing HeLa cells with PBMCs and ZnO-NPs in 6-well plates with 2 mL of fresh cell culture medium for 24 hours at 37°C under 5% CO₂.

After incubation, the supernatant was collected and centrifuged. The pellet was resuspended in 500 μ L of buffer solution and gently pipetted. Annexin V-FITC (2 μ L) was added to each sample and incubated in the dark

for 15 minutes. Following this, 2 μ L of PI reagent was added, and cell apoptosis was analyzed using a FACSCalibur flow cytometer (BD Biosciences, USA). Data analysis was conducted with FlowJo software (version 10.10, Tree Star, USA).

During analysis, cells positive for Annexin V-FITC but negative for PI were classified as early apoptotic cells, while those positive for both Annexin V-FITC and PI were identified as late apoptotic cells. Additionally, cells negative for Annexin V-FITC but positive for PI were categorized as necrotic cells.

Statistical Analysis

Relative quantification was performed using the $2^{-\Delta\Delta Ct}$ method. Statistical analyses were performed using SPSS version 26.0 (SPSS Inc., Chicago, IL, USA), and GraphPad Prism version 9.0 (GraphPad, La Jolla, CA, USA) was used for presenting the results. The normality of the data was evaluated by the Kolmogorov–Smirnov test. For group comparisons, the two-tailed Mann–Whitney U test was utilized. Gene expression results were reported as mean \pm SD and fold change (FC). A *p*-value less than 0.05 was considered statistically significant.

RESULTS

Characterization of ZnO-NPs

The intensity-weighted size distribution revealed a Z-average diameter of 181.1 nm with a polydispersity index (PdI) of 0.404. The count rate during measurement was 181.1 kcps, ensuring reliable data acquisition. Three size peaks were recorded; however, Peak 1 (132.7 nm) contributed 100% intensity, suggesting a single nanoparticle population (Figure 1). However, the relatively elevated PdI value indicates a moderate degree of size heterogeneity, which may be attributable to partial particle aggregation during or after synthesis.

FE-SEM revealed nearly spherical particles with an average diameter of 60–100 nm. Mostly, these ZnO nanospheres were bound together to create aggregates (Figures 2A and 2B). Furthermore, according to EDS patterns and element weight percentages, Zn and O elements were found to be present in a specific weight ratio of 79.55% and 20.45%, respectively (Figure 2C). The yellow and red dots in the EDS elemental mapping showed that the Zn and O elements in the ZnO-NPs were distributed rather uniformly (Figure 2D).

Effects of ZnO Nanoparticles in a PBMC–HeLa Co-culture

	Diam. (nm)	% Intensity	Width (nm)
Z-Average (r.nm): 181.1	Peak 1: 132.7	100.0	36.03
PdI: 0.404	Peak 2: 0.000	0.0	0.000
Intercept: 0.764	Peak 3: 0.000	0.0	0.000
Result quality Refer to quality report			

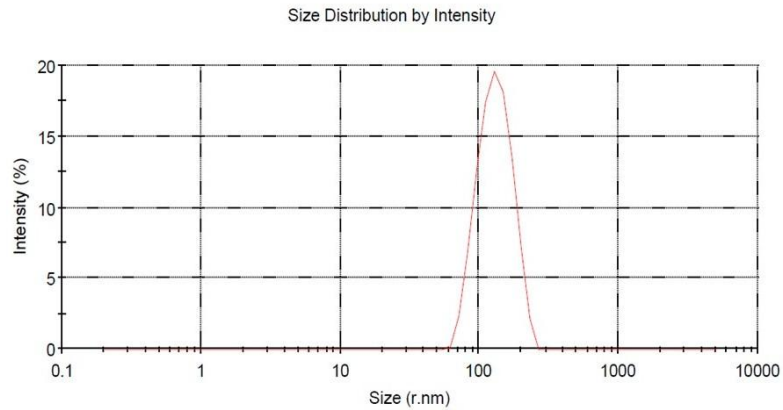


Figure 1. Hydrodynamic size distribution of Zinc oxide nanoparticles (ZnO-NPs) measured by dynamic light scattering (DLS). The intensity-weighted size distribution shows a Z-average diameter of 181.1 nm with a polydispersity index (PdI) of 0.404, indicating a moderately heterogeneous nanoparticle population. The dominant peak corresponds to a single particle population with an average size of 132.7 nm.

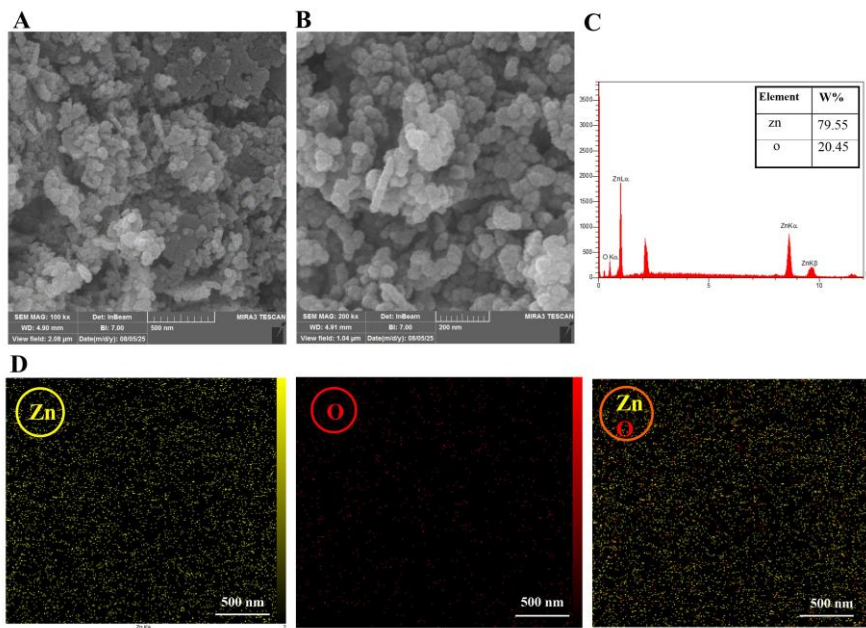


Figure 2. Morphological and elemental characterization of Zinc oxide nanoparticles (ZnO-NPs). (A and B) Field emission scanning electron microscopy (FE-SEM) images of ZnO-NPs at different magnifications, showing predominantly spherical nanostructures with partial aggregation, (C) Energy-dispersive X-ray spectroscopy (EDS) spectrum confirms the presence of zinc (Zn) and oxygen (O) with corresponding weight percentages, (D) Elemental mapping images demonstrating the homogeneous distribution of Zn and O within the nanoparticle structure.

Cytotoxicity Assay

Based on the results of the 24-hour MTT assay, HeLa cells exhibit an IC_{50} value of 7 $\mu\text{g/mL}$, reflecting a high sensitivity to ZnO-NPs. In contrast, PBMCs display an IC_{50} value of 40 $\mu\text{g/mL}$, indicating significantly lower sensitivity to these NPs (Figure 3).

The high IC_{50} value for PBMCs suggests that their viability remains largely unaffected even at elevated concentrations of ZnO-NPs after 24 hours. Conversely, the low IC_{50} value for HeLa cells demonstrates their pronounced sensitivity, with substantial cell death occurring at relatively low concentrations within the same timeframe.

Collectively, these findings indicate that ZnO-NPs have a selective cytotoxic effect, with a significantly higher susceptibility in cancerous HeLa cells than in normal PBMCs.

Cytokine Analysis

The gene expression analysis revealed that the expression levels of *IL1B*, *IL2*, *IL4*, *TNF*, *TGFB1*, and *IFNG* in PBMCs were significantly higher in the HeLa/PBMCs and HeLa/PBMCs/ZnO groups compared to the Ctrl group ($p < 0.01$). Further analysis demonstrated that the expression levels of *IL1B*, *TNF*, *TGFB1*, and *IFNG* were significantly elevated in the HeLa/PBMCs/ZnO group compared to the HeLa/PBMCs group ($p < 0.01$). However, no significant

differences were observed between these two groups in the expression levels of *IL2* and *IL4* (Figure 4).

Overall, our findings suggest that ZnO-NPs may boost the immune response in the co-culture model, especially by increasing the production of pro-inflammatory (*IL1B*, *TNF*, and *IFNG*) and regulatory (*TGFB1*) cytokines while having no effect on *IL2* and *IL4* levels. Instead of a non-specific immune activation, this pattern points to a targeted regulation of cytokine signaling pathways.

Angiogenesis Analysis

Co-culture of HeLa cells with PBMCs significantly reduced *VEGFA* expression compared to the control ($p < 0.01$). Further treatment with ZnO-NPs in the HeLa/PBMC group resulted in a marked decrease in *VEGFA* expression ($p < 0.01$). ZnO-NPs treatment of HeLa cells alone (HeLa/ZnO) also showed a reduction in *VEGFA* expression compared to the control, but the decrease was less than in the HeLa/PBMC/ZnO group (Figure 5).

Taken together, these results indicate that ZnO-NPs inhibit angiogenesis-related signaling, evidenced by the downregulation of *VEGFA* expression. The greater reduction of *VEGFA* expression in the HeLa/PBMC/ZnO group suggests a synergistic interaction between PBMC-mediated immune responses and NP treatment in reducing pro-angiogenic activity.

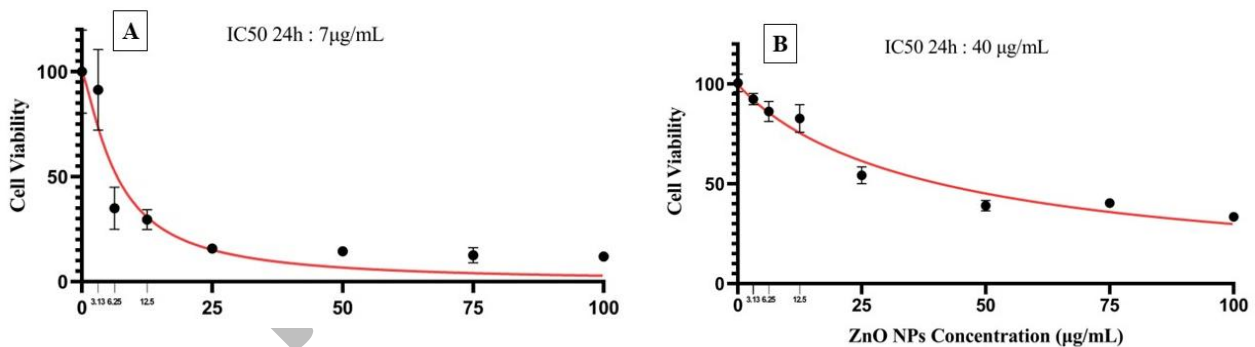


Figure 3. Cytotoxic effects of ZnO nanoparticles (ZnO-NPs) on HeLa cells and peripheral blood mononuclear cells (PBMCs) after 24 hours of exposure. (A) Dose–response curve of HeLa cells treated with increasing concentrations of ZnO-NPs (0, 3.13, 6.25, 12.5, 25, 50, 75, and 100 $\mu\text{g/mL}$), showing an IC_{50} value of 7 $\mu\text{g/mL}$. (B) Dose–response curve of PBMCs exposed to the same concentration range, demonstrating lower sensitivity to ZnO-NPs with an IC_{50} value of 40 $\mu\text{g/mL}$ (Half maximal inhibitory concentration: IC_{50}).

Effects of ZnO Nanoparticles in a PBMC–HeLa Co-culture

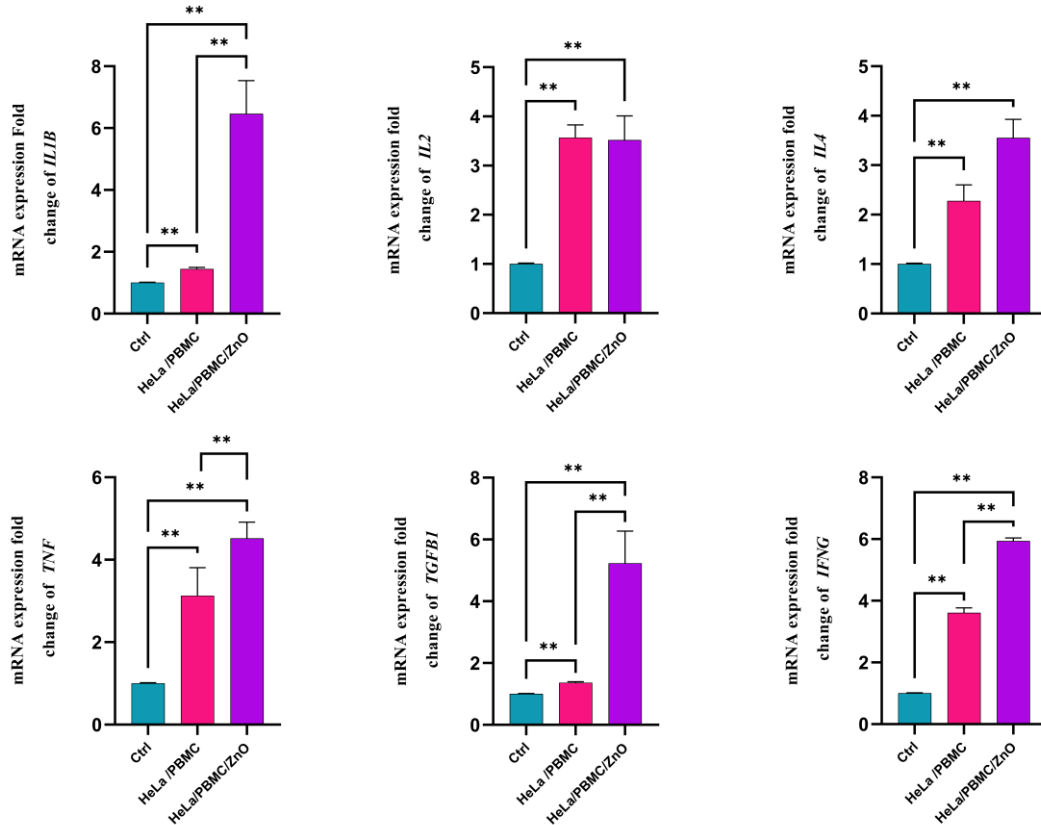


Figure 4. Relative mRNA expression levels of cytokines in PBMCs.

The fold change in mRNA expression of *IL1B*, *IL2*, *IL4*, *TNF*, $TGF-\beta$, *IFNG* in PBMCs between Ctrl, HeLa/PBMCs, and HeLa/PBMCs/ZnO groups (PBMC: peripheral blood mononuclear cells, ZnO: Zinc oxide, *IL1B*: interleukin 1 beta, *IL2*: interleukin 2, *IL4*: interleukin 4, *TNF*: tumor necrosis factor, *TGFβ1*: transforming growth factor beta 1, *IFNG*: and interferon gamma, **: $p < 0.01$).

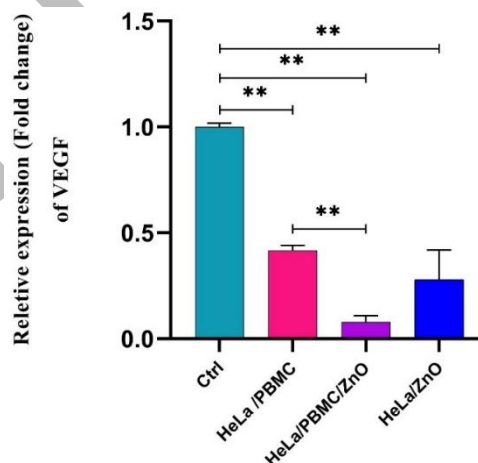


Figure 5. Relative mRNA expression of *VEGFA* in different experimental groups following zinc oxide treatment.

Comparison of mRNA expression fold change of *VEGFA* between Ctrl, HeLa/PBMCs, HeLa/PBMCs/ZnO, and HeLa/ZnO groups. The reduction in *VEGFA* expression reflects the inhibitory effect of ZnO-NPs and immune cell co-culture on angiogenesis-related signaling (PBMC: peripheral blood mononuclear cells, *VEGFA*: Vascular endothelial growth factor, ZnO: Zinc oxide, **: $p < 0.01$).

Apoptosis

Apoptosis analysis revealed a significant increase in apoptosis of HeLa cells in the HeLa/PBMCs, HeLa/PBMCs/ZnO, and HeLa/ZnO groups compared to the Ctrl group ($p<0.05$). Among these groups, apoptosis

in the co-culture of HeLa/PBMCs/ZnO was significantly higher than in both the HeLa/PBMCs and HeLa/ZnO groups ($p<0.05$). However, no significant difference was observed between the HeLa/PBMCs group and the HeLa/ZnO group (Figure 6).

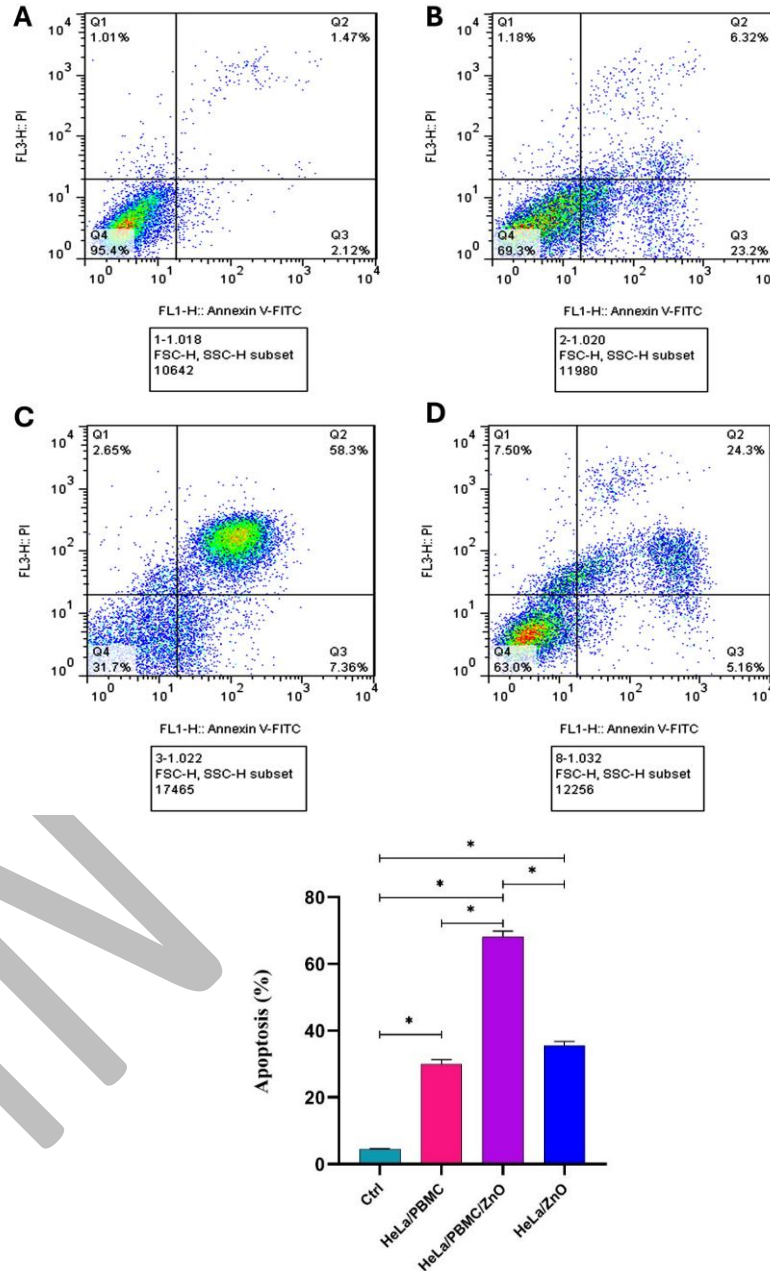


Figure 6. Flowcytometry analysis of the impact of ZnO on apoptosis of HeLa cells
 HeLa cells were co-cultures with PBMCs and the effect of ZnO on early and late apoptosis was evaluated by flow cytometry. The percentage of apoptotic cells was significantly increased in the HeLa/PBMC/ZnO group compared with other groups. (PBMC: peripheral blood mononuclear cells, ZnO: Zinc oxide, *: $p<0.05$).

The data highlight a significant increase in apoptosis of HeLa cells upon exposure to ZnO-NPs, with the greatest effect observed when co-cultured with PBMCs. This synergistic induction of apoptosis highlights the potential application of using NPs together with immune cells to improve anti-cancer effectiveness.

DISCUSSION

In this study, we investigated the immunomodulatory and anti-cancer effects of ZnO-NPs in a HeLa/PBMC co-culture model. Our results demonstrated that ZnO-NPs significantly reduced HeLa cell viability, enhanced their apoptosis, modulated the expression of key inflammatory cytokines, and suppressed angiogenic signaling. These findings highlight the importance of immune–tumor interactions in shaping the biological effects of ZnO-NPs.

ZnO-NPs have attracted attention as potential anti-cancer agents due to their biocompatibility and rather selective cytotoxicity toward rapidly proliferating cancer cells. Their selective cytotoxicity toward proliferative cells, compared to non-proliferative counterparts, further enhances their potential as effective nanocarriers in cancer therapy.¹⁵⁻¹⁸

The use of ZnO-NPs in cancer treatment has captured the attention of researchers, with numerous studies published illustrating their anti-cancer properties against various cancer types and different cell lines including liver cancer (HepG2),¹⁹⁻²¹ lung cancer (A549),^{20,22-24} breast cancer (MCF-7),²⁵⁻²⁷ bone cancer (MG-63),²⁸ colon cancer (Caco-2, HCT-116, HT-29),²⁹⁻³² human multiple myeloma (RPMI8226),³³ myoblast cell line (C2C12),³⁴ oral cancer (CAL27),³⁵ gastric cancer (MGC803),³⁶ rhabdomyosarcoma cell line,³⁷ laryngeal cancer (Hep-2),¹⁸ human brain tumor (U87),³⁸ ovarian cancer (SKOV3),^{39, 40} melanoma cancer (Cloudman),⁴¹ and gingival squamous cell carcinoma (Ca9-22 and OECM-1).⁴²

Notably, several reports suggest that ZnO-NPs may exert greater cytotoxic effects on malignant cells than on PBMCs at comparable concentrations, indicating a degree of tumor selectivity.⁴³

Consistent with our findings, several studies have reported the cytotoxic effects of ZnO-NPs, either alone or in combination with other nanomaterials, on HeLa cells.⁴⁴⁻⁴⁶ However, studies investigating ZnO-NP-induced cytotoxicity in co-culture systems with PBMCs

are still limited. Therefore, our co-culture model offers additional insight into how immune cells could influence ZnO-NP-induced cytotoxic responses in cervical cancer cells.

The morphology and elemental composition of the synthesized ZnO-NPs were in accordance with previously documented findings.^{47,48} The consistent physical and chemical characteristics of nanoparticles influence cellular interactions and biological responses, consequently supporting the idea that the observed effects are related to exposure to ZnO-NPs rather than experimental variations.

Gene expression analysis revealed a significant upregulation of pro-inflammatory cytokines (including *IL1B*, *TNF*, *IFNG*), and *TGFB1* as a pleiotropic cytokine in the HeLa/PBMCs/ZnO group, compared to the HeLa/PBMCs group, indicating strong activation of innate and adaptive immune pathways. This cytokine profile suggests that ZnO-NPs can potentiate immune-mediated anti-tumor responses within the co-culture environment. The presence of PBMCs in the co-culture system likely contributes to this response by enabling immune–tumor cross-talk that amplifies cytokine signaling. It should be noted that these findings are based on mRNA expression levels, and changes in gene expression may not necessarily translate directly into protein secretion or functional immune responses.

The impact of ZnO-NPs on cytokine production has only been assessed in a limited number of studies, and the majority of these have been performed in immortalized and nonhematological cell lines, which frequently exhibit changes in signal transduction pathways that result in unpredictable changes in protein expression.⁴⁹ Research has shown that some nanomaterials may increase the production of cytokines in PBMCs; however, it depends on a number of variables, including the material's composition, size, and delivery method.⁵⁰⁻⁵² In both in vitro and in vivo models, ZnO-NPs exposure has been associated with increased production of pro-inflammatory cytokines such as *TNF* and *IFNG*, supporting their capacity to trigger immune activation under specific conditions.^{49,53,54}

We found that ZnO-NPs induces the production of pro-inflammatory cytokines at even very low concentrations, which were below those concentrations that caused cell death. This finding suggests that, if ZnO is utilized at proper concentrations, it could accelerate tumor cell killing by producing *TNF*, a cytokine known

for its potent anti-tumor properties.⁵⁵ For example, a previous study showed that factors such as higher age and exposure to ZnO-NPs may play role in serum level of inflammatory variables. For example, following exposure with ZnO-NPs, blood levels of interleukin 1 (IL-1) and interleukin 6 (IL-6) were markedly elevated in both adult and elderly groups when compared to the corresponding control groups of the same age.⁵⁶ Another investigation revealed that ZnO-NPs significantly increased *IFNG* and *TNF* levels in a dose-dependent pattern. On the other hand, ZnO-NPs alone did not stimulate *interleukin 12 (IL12)* synthesis in unprimed cells; however, pretreatment with low concentrations of interferon gamma (IFN- γ) resulted in a concentration-dependent increase in IL-12. These results suggest a synergistic interaction between ZnO-NPs and IFN- γ , underscoring the potential of ZnO-NPs in initiating a critical inflammatory response.⁵¹

The elevated production of *IL1B*, *IFNG*, *TNF*, and *IL2* identified in the present study in accordance with previous findings suggest that ZnO-NPs might augment Th1-associated immune responses, which are essential for effective cell-mediated antitumor immunity. The simultaneous upregulation of *TGFB1* and pro-inflammatory cytokines may indicate its context-dependent immunoregulatory function within TME, where *TGFB1* signaling can dynamically influence immune activation, cellular interactions, and tissue remodeling, rather than just acting as an immunosuppressive pathway, especially in immune-infiltrated environments.^{57,58}

In contrast, transcriptomics-based analysis of the toxicity of ZnO-NPs on chronic myeloid leukemia cells revealed that the treated cells produced less cytokines. This was shown by the downregulation of 41 genes in the treated cells, in addition to 17 genes encoding cytokines or cytokine receptors.⁴³ It has been shown that *TGFB1* synthesis in different cell types is influenced by ZnO-NPs. For example, exposure to ZnO-NPs decreased *TGFB1* expression at the mRNA and protein levels in murine photoreceptor-derived cells (661W) in a concentration-dependent manner.⁵⁹ Moreover, an increased level of *IL2*, *IL4*, *IL6*, and *interleukin 17 (IL17)* in splenocytes administered with ZnO-NPs was observed in comparison with the control.⁶⁰ However, the ZnO-NP-associated increase in *IL4* and *TGFB1* observed in the present HeLa/PBMC co-culture model appears to be less explored in cancer models, so the effects of ZnO-NPs on other cytokines and in co-culture

systems with HeLa cells require further investigation for definitive conclusions.⁶¹

Overall, these results indicate that ZnO-NPs can change cytokine responses differently based on the experimental model and cellular environment, with co-culture systems offering a more physiologically reliable representation of immune-tumor interactions. Nonetheless, the current study had specific limitations that must be acknowledged when interpreting the findings. The limited number of donors and experimental replicates, a common limitation in exploratory in vitro co-culture experiments, indicates that the results should be considered preliminary. Subsequent research using larger sample sizes and supplementary validation methods is necessary to confirm these findings.

Furthermore, this study highlighted a synergistic effect of ZnO-NPs in promoting cancer cell apoptosis following HeLa/PBMC co-culture, with the highest rates in the HeLa/PBMCs/ZnO group. In vitro co-culture models, involving tumor cells and PBMCs, are valuable for studying the interactions between immune and cancer cells. However, specific studies examining the effects of ZnO-NPs in co-culture systems of PBMCs with HeLa or other tumor cells are limited. The immunological microenvironment, including interactions with PBMCs, may have an impact on the oxidative stress and apoptotic pathways triggered by ZnO-NPs, according to the data currently available. ZnO-NPs cause mitochondrial depolarization and reactive oxygen species (ROS) production in HeLa cells, which can promote their apoptosis. PBMCs may influence this reaction in co-culture and affect the degree or mode of apoptosis.⁶²⁻⁶⁴

ZnO-NPs have been shown to induce cytotoxicity through the production of ROS, via pathways involving p53, leading to apoptosis in cancer cells.⁶⁵ Plant-based ZnO-NPs also demonstrated selective cytotoxicity against HeLa cells, significantly reducing cell viability.⁶⁶ Earlier studies also reported that nanostructure treatment at concentrations exceeding 15.6 $\mu\text{g/mL}$ exerts synergistic cytotoxic effects on HeLa cells, primarily through apoptosis induction, proliferation reduction, and promotion of cell death in a concentration-dependent manner.⁶⁷ Increased apoptosis in HepG2 cells has been observed following nanoparticle treatment, consistent with earlier reports demonstrating that green-synthesized ZnO-NPs can effectively induce apoptosis in HeLa cells.⁶⁸ Biosynthesized silver nanoparticles

have also been shown to enhance apoptotic pathways in the MCF-7 breast cancer cell line.⁶⁹ Moreover, iron oxide nanoparticles have been reported to induce cell cycle arrest and apoptosis in Jurkat, MCF-7, and HepG2 cells.⁷⁰ Similarly, ZnO-NPs result in cell death by induction of apoptosis in HepG2 and MCF-7 cancer cells.¹⁷

Further studies showed that ZnO-NPs, including chitosan-coated forms, significantly increase apoptosis in cervical cancer cells. This is associated with elevated ROS production and decreased antioxidant activity, potentially due to excess dissolved zinc ions, which triggers apoptosis. Key apoptotic proteins such as p53, Bax, caspase-3, caspase-9, and cytochrome-c are involved, while anti-apoptotic proteins like Bcl-2 are downregulated.^{71,72}

In this study, flow cytometry analysis demonstrated significant increases in early and late apoptotic HeLa cells after incubation with ZnO-NPs, accompanied by upregulation of mRNA levels of apoptotic markers. Additionally, ZnO-NPs can induce apoptosis through mitochondrial pathways and DNA damage.^{73,74}

Based on the outcomes of angiogenesis analysis, the expression levels of *VEGFA*, a key mediator of tumor vascularization, were significantly reduced in the HeLa/PBMCs/ZnO group compared to other groups. This underscores the potential of ZnO-NPs to inhibit angiogenic signaling, which is crucial for tumor growth and metastasis. In line with our findings, previous studies have demonstrated that ZnO-NPs can modulate tumor angiogenesis pathways under various experimental conditions, further supporting their anti-angiogenic and anti-cancer properties.^{75,76} Anti-angiogenic effects of ZnO-NPs have also been reported in other tumor models; however, the observed outcomes appear to be highly dependent on experimental conditions and nanoparticle concentration.⁷⁷

Overall, the present study provides observational evidence that ZnO-NPs may influence immune-related and angiogenesis-associated responses in a HeLa/PBMC co-culture setting. In this context, the use of a co-culture model offers a more physiologically relevant context than monoculture systems.

This study highlights the potential of ZnO-NPs as a multi-functional therapeutic agent for the treatment of cancer, namely in the HeLa/PBMC co-culture model. ZnO-NPs demonstrated notable apoptotic induction, suppression of angiogenic markers, and modulation of cytokines levels, all of which can contribute in anti-

tumor effects. These findings underscore the dual capacity of ZnO-NPs to target cancer cells while enhancing immune responses. Therefore, more mechanistic investigations and preclinical assessments are required to enhance their clinical application and validate their safety profile.

STATEMENT OF ETHICS

The present study was approved under the ethics code IR.BMSU.BLC.1403.065 by the Research Ethics Committees of Biosafety & Laboratory, Baqiyatallah University of Medical Sciences, Tehran, Iran.

FUNDING

Not applicable.

CONFLICT OF INTEREST

The authors declare no conflicts of interest.

ACKNOWLEDGMENTS

Thanks to guidance and advice from "Clinical Research Development Unit of Baqiyatallah Hospital". We would like to thank the guidance and support from Research and Technology Comprehensive Laboratory (RTCL) of Baqiyatallah University of Medical Sciences. The authors acknowledge the scientific and technical support of the Molecular Biology Research Center, Systems Biology and Poisoning Institute, Baqiyatallah University of Medical Sciences, Tehran, Iran. The authors also acknowledge as well as the scientific assistance of the Department of Immunology, School of Medicine, Iran University of Medical Sciences, Tehran, Iran.

DATA AVAILABILITY

Applicable.

AI ASSISTANCE DISCLOSURE

No artificial intelligence (AI) tools were used in the preparation of this manuscript.

REFERENCES

- Small W Jr, Bacon MA, Bajaj A, Chuang LT, Fisher BJ, Harkenrider MM, et al. Cervical cancer: a global health crisis. *Cancer*. 2017;123(13):2404–12.
- Maio M, Ascierto PA, Manzyuk L, Motola-Kuba D, Penel N, Cassier PA, et al. Pembrolizumab in microsatellite instability–high or mismatch repair–deficient cancers: updated analysis from the phase II KEYNOTE-158 study. *Ann Oncol*. 2022;33(9):929–38.
- Monk BJ, Colombo N, Oza AM, Fujiwara K, Birrer MJ, Randall L, et al. First-line pembrolizumab plus chemotherapy versus placebo plus chemotherapy for persistent, recurrent, or metastatic cervical cancer: final overall survival results of KEYNOTE-826. *J Clin Oncol*. 2023;41(36):5505–11.
- Zivyar N, Pourmortazavi SM, Taghdiri M, Rahimi Kalateh Shah Mohammad G, Saboury AA, Falahati M. Evaluation of green synthesis, characterization and antibacterial activity of silver nanoparticles from *Crocus sativus* corm extract. *J Hortic Postharvest Res*. 2021;4(Spec Iss):19–32.
- Ratan ZA, Haidere MF, Nurunnabi M, Shahriar SM, Ahammad AJ, Shim YB, et al. Green chemistry synthesis of silver nanoparticles and their potential anticancer effects. *Cancers (Basel)*. 2020;12(4):855.
- Jayaseelan C, Rahuman AA, Kirthi AV, Marimuthu S, Santhoshkumar T, Bagavan A, et al. Novel microbial route to synthesize ZnO nanoparticles and their activity against pathogenic bacteria and fungi. *Spectrochim Acta A Mol Biomol Spectrosc*. 2012;90:78–84.
- Chung IM, Rahuman AA, Marimuthu S, Kirthi AV, Anbarasan K, Rajakumar G. Cytotoxicity and caspase-mediated apoptotic effect of green synthesized zinc oxide nanoparticles on human liver carcinoma cells. *Nanomaterials (Basel)*. 2015;5(3):1317–30.
- Wiesmann N, Tremel W, Brieger J. Zinc oxide nanoparticles for therapeutic purposes in cancer medicine. *J Mater Chem B*. 2020;8(23):4973–89.
- Mishra PK, Mishra H, Ekielski A, Talegaonkar S, Vaidya B. Zinc oxide nanoparticles: a promising nanomaterial for biomedical applications. *Drug Discov Today*. 2017;22(12):1825–34.
- Zhang ZY, Xiong HM. Photoluminescent ZnO nanoparticles and their biological applications. *Materials (Basel)*. 2015;8(6):3101–27.
- Reichel D, Tripathi M, Perez JM. Biological effects of nanoparticles on macrophage polarization in the tumor microenvironment. *Nanotheranostics*. 2019;3(1):66–88.
- Yi M, Zhang J, Li A, Niu M, Yan Y, Jiao Y, et al. Targeting cytokine and chemokine signaling pathways for cancer therapy. *Signal Transduct Target Ther*. 2024;9(1):176.
- Jou E. Type 1 and type 2 cytokine-mediated immune orchestration in the tumour microenvironment and their therapeutic potential. *Explor Target Antitumor Ther*. 2023;4(3):474–97.
- Lee C, Lee J, Choi J, Park S, Kim Y, Kim H, et al. Vascular endothelial growth factor signaling in health and disease. *Signal Transduct Target Ther*. 2025;10(1):170.
- Selvakumari D, Deepa R, Mahalakshmi V, Subhashini P, Lakshmi PT. Anticancer activity of ZnO nanoparticles on MCF-7 and A549 cancer cell lines. *ARPN J Eng Appl Sci*. 2015;10(12):5418–22.
- Valdiglesias V, Costa C, Sharma V, Kilic G, Pasaro E, Teixeira JP, et al. Neuronal cytotoxicity and genotoxicity induced by zinc oxide nanoparticles. *Environ Int*. 2013;55:92–100.
- Wahab R, Kim YS, Mishra A, Yun SI, Shin HS. ZnO nanoparticles induced oxidative stress and apoptosis in HepG2 and MCF-7 cancer cells. *Colloids Surf B Biointerfaces*. 2014;117:267–76.
- Wang Y, Zhang S, Wei X, Zhang X, Zhang J. Synthesis of zinc oxide nanoparticles inhibits proliferation and induces apoptosis in laryngeal cancer cells. *J Photochem Photobiol B*. 2019;201:111624.
- Abbasi BA, Iqbal J, Ahmad R, Zia L, Kanwal S, Mahmood T. Bioactivities of Geranium wallichianum leaf extracts conjugated with zinc oxide nanoparticles. *Biomolecules*. 2019;10(1):38.
- Hussain A, Oves M, Alajmi MF, Hussain I, Amir S, Ahmed FJ, et al. Biogenesis of ZnO nanoparticles using Pandanus odorifer leaf extract: anticancer and antimicrobial activities. *RSC Adv*. 2019;9(27):15357–69.
- Rahimi Kalateh Shah Mohammad G, Saboury AA, Falahati M, Mahdih Z, Gharavi S. Cytotoxic properties of zinc oxide nanoparticles and anticancer impacts. *J Biochem Mol Toxicol*. 2019;33(7):e22324.
- Hira I, Ahmad M, Arshad M, Ali A, Abbasi BH. Pectin–guar gum–zinc oxide nanocomposite enhances cytotoxicity towards lung and breast carcinomas. *Mater Sci Eng C*. 2018;90:494–503.
- Rajeshkumar S, Malarkodi C, Vanaja M, Annadurai G. Biosynthesis of zinc oxide nanoparticles using *Mangifera indica* leaves and cytotoxic properties in A549 cells. *Enzyme Microb Technol*. 2018;117:91–5.
- Umamaheswari A, Prabu SL, Puratchikody A. Green synthesis of zinc oxide nanoparticles and anticancer

- activity in A549 cells. *Biotechnol Rep (Amst)*. 2021;29:e00595.
25. Malaikozhundan B, Vaseeharan B, Vijayakumar S, Pandiselvi K, Kalanjiam R, Murugan K, et al. Pongamia pinnata-coated zinc oxide nanoparticles against pathogens and breast cancer cells. *Microb Pathog*. 2017;104:268–77.
 26. Prasad KS, Pathak D, Patel A, Dalwadi P, Prasad R, Patel P. Antitumor potential of green synthesized ZnO nanoparticles against breast cancer cells. *Separations*. 2021;8(1):8.
 27. Sadhukhan P, Kundu M, Chatterjee S, Ghosh N, Manna P, Das J, et al. Targeted delivery of quercetin via pH-responsive zinc oxide nanoparticles for breast cancer therapy. *Mater Sci Eng C*. 2019;100:129–40.
 28. Cheng J, Zhang S, Wang L, Wang Z, Wu Y. Green synthesized zinc oxide nanoparticles regulate apoptotic expression in MG-63 cells. *J Photochem Photobiol B*. 2020;202:111644.
 29. Ahlam AA, Al-Hazmi F, Al-Ghamdi AA, Alnowaiser F, Alarfaj N, Siddiqui MRH, et al. Zinc oxide nanoparticles induce apoptotic–necrotic death in cancer cells. *Biol Trace Elem Res*. 2021;199:1778–801.
 30. Dulta K, Thakur A, Kaushal J, Chauhan PK. Synthesis of zinc oxide nanoparticles using *Bergenia ciliata* and anticancer potential. *J Inorg Organomet Polym Mater*. 2021;31:180–90.
 31. El-Belely EF, Farag MM, Said HA, Amin AS, Azab E, Gobara M, et al. Green synthesis of zinc oxide nanoparticles and biomedical activities. *Nanomaterials (Basel)*. 2021;11(1):95.
 32. Selim YA, Azb MA, Ragab I, El-Ahmady RM. Green synthesis of zinc oxide nanoparticles and cytotoxic activities. *Sci Rep*. 2020;10(1):3445.
 33. Li Z, Huang J, Wu Y, Guo Y, Liu M, Xu Y, et al. Zinc oxide nanoparticles induce multiple myeloma cell death via ROS-mediated signaling. *Biomed Pharmacother*. 2020;122:109712.
 34. Wahab R, Khan F, Mishra YK, Musarrat J, Al-Khedhairi AA. Zinc oxide quantum dots induce apoptosis via caspase activation. *RSC Adv*. 2016;6(31):26111–20.
 35. Wang J, Deng X, Zhang F, Chen D, Ding W, Zhang Y, et al. Zinc oxide nanoparticles activate mitophagy in oral cancer cells. *Int J Nanomedicine*. 2018;13:3441–50.
 36. Bi C, Li L, Wang Z, Zhou Y, Wang H, Liu Y. Biofabrication of zinc oxide nanoparticles and cytotoxicity toward gastric cancer cells. *Biomed Res*. 2017;28:2065–9.
 37. Perera W, Hewavitharana AK, Navaratne SB, Wickramasinghe S, Fernando SSN, Rajapakse RPVJ. Curcumin-loaded zinc oxide nanoparticles for enhanced anticancer activity. *RSC Adv*. 2020;10(51):30785–95.
 38. Wahab R, Kim YS, Mishra A, Yun SI, Shin HS. Cytotoxic effect of ZnO nanostructures on brain and cervical cancer cells. *JBIC J Biol Inorg Chem*. 2011;16:431–42.
 39. Bai DP, Zhang XF, Zhang GL, Huang YF, Gurunathan S. Zinc oxide nanoparticles induce apoptosis and autophagy in ovarian cancer cells. *Int J Nanomedicine*. 2017;12:6521–35.
 40. Padmanabhan A, Khan A, Najafabadi AH, Khan N, Khan I, Zubair M, et al. Zinc oxide nanoparticles trigger apoptosis in ovarian cancer cells. *Appl Surf Sci*. 2019;487:807–18.
 41. Wahab R, Khan F, Yang YB, Hwang IH, Shin HS. ZnO nanoparticles induce oxidative stress in melanoma cells. *J Biomed Nanotechnol*. 2013;9(3):441–9.
 42. Wang SW, Lee CH, Lin MS, Chi CW, Chen YC, Wang YJ, et al. ZnO nanoparticles induce apoptosis in gingival carcinoma cells. *Int J Mol Sci*. 2020;21(5):1612.
 43. Alsagaby SA, Khan M, Mousa RA, Abd-Elkader OH, Al-Otaibi F, Ahmed F, et al. Transcriptomics-based characterization of ZnO nanoparticle toxicity. *Int J Nanomedicine*. 2020;15:7901–21.
 44. AbuMousa RA, Alsagaby SA, Alshahrani MY, Mousa SA, Khan M. Photocatalytic effects of WO₃/ZnO nanocomposite on HeLa cells. *Saudi J Biol Sci*. 2020;27(7):1743–52.
 45. Dillip GR, Reddy TS, Sadanandam G, Reddy NS, Reddy VR. In vitro cytotoxicity of zinc oxide–anchored nanofibers on HeLa cells. *Mater Sci Semicond Process*. 2017;59:87–92.
 46. Sirelkhatim A, Mahmud S, Seeni A, Kaus NHM, Ann LC, Bakhori SKM, et al. Preferential cytotoxicity of ZnO nanoparticles toward cervical cancer cells. *J Nanopart Res*. 2016;18:1–17.
 47. Aghazadeh-Ghomi M, Pourabbas Z. Rapid synthesis of zinc oxide nanoparticles via precipitation. *J Mater Sci Mater Electron*. 2021;32(19):24363–8.
 48. Mohanasundaram P, Saral MA. Biological applications of green synthesized ZnO nanoparticles from neem flower. *Sci Rep*. 2025;15(1):17727.
 49. Gojova A, Guo B, Kota RS, Rutledge JC, Kennedy IM, Barakat AI. Inflammation induced by metal oxide nanoparticles. *Environ Health Perspect*. 2007;115(3):403–9.
 50. Duffin R, Tran L, Brown D, Stone V, Donaldson K. Proinflammatory effects of metal nanoparticles. *Inhal Toxicol*. 2007;19(10):849–56.

51. Hanley C, Layne J, Punnoose A, Reddy KM, Coombs I, Coombs A, et al. Influence of ZnO nanoparticle size on immune cell cytotoxicity. *Nanoscale Res Lett.* 2009;4(12):1409–20.
52. Sayes CM, Reed KL, Warheit DB. Toxicity assessment of fine and nanoparticles. *Toxicol Sci.* 2007;97(1):163–80.
53. Beyerle A, Irmeler M, Beckers J, Kissel T, Stoeger T. Screening strategy to avoid toxicological hazards of nanoparticles. *J Phys Conf Ser.* 2009;170:012003.
54. Hanley C, Thurber A, Hanna C, Punnoose A, Zhang J, Wingett DG. Size-dependent cytotoxicity of zinc oxide nanoparticles. *Nanoscale Res Lett.* 2009;4:1409–20.
55. Rasmussen JW, Martinez E, Louka P, Wingett DG. Zinc oxide nanoparticles for selective tumor cell destruction. *Expert Opin Drug Deliv.* 2010;7(9):1063–77.
56. Tian L, Lin B, Wu L, Li K, Liu H, Yan J, et al. Neurotoxicity induced by zinc oxide nanoparticles. *Sci Rep.* 2015;5:16117.
57. Batlle E, Massagué J. Transforming growth factor- β signaling in immunity and cancer. *Immunity.* 2019;50(4):924–40.
58. Pickup M, Novitskiy S, Moses HL. Roles of TGF- β in the tumour microenvironment. *Nat Rev Cancer.* 2013;13(11):788–99.
59. Guo DD, Li W, Zhang H, Zhang X, Zhang J, Wang Y, et al. ZnO nanoparticles inhibit cell proliferation via TGF- β reduction. *Cell Prolif.* 2015;48(2):198–208.
60. Roy R, Singh SK, Das M, Tripathi A, Dwivedi PD. Adjuvant effect of zinc oxide nanoparticles. *Int Immunol.* 2014;26(3):159–72.
61. Folkman J. Tumor angiogenesis: therapeutic implications. *N Engl J Med.* 1971;285(21):1182–6.
62. Sharma V, Anderson D, Dhawan A. Zinc oxide nanoparticles induce oxidative DNA damage in HepG2 cells. *Apoptosis.* 2012;17(8):852–70.
63. Wang J, Deng X, Zhang F, Chen D, Ding W, Zhang Y, et al. ZnO nanoparticle-induced apoptosis via JNK signaling. *Nanoscale Res Lett.* 2014;9(1):117.
64. Kulkarni BD, Ramesh V, Reddy MS, Veeranjanyulu A, Ramesh B, Rao KN. Cytotoxicity of zinc nanoparticles on HeLa cells. *Pharmacogn J.* 2016;8(2):1–6.
65. Miri A, Sarani M, Zarrabi A, Rahimi M, Alizadeh S. Zinc oxide nanoparticles: biosynthesis and cytotoxic activity. *Mater Sci Eng C Mater Biol Appl.* 2019;104:109981.
66. Nagajyothi PC, Cha SJ, Yang IJ, Sreekanth TVM, Kim KJ, Shin HM. Green synthesis of copper oxide nanoparticles and anticancer activity. *Arab J Chem.* 2017;10(2):215–25.
67. Kulandaivelu B, Gothandam K. Cytotoxic effect of biologically synthesized silver nanoparticles. *Braz Arch Biol Technol.* 2016;59:e16150529.
68. Namvar F, Rahman HS, Mohamad R, Baharara J, Mahdavi M, Amini E, et al. Cytotoxic effect of magnetic iron oxide nanoparticles. *Int J Nanomedicine.* 2014;9:2479–88.
69. Chen H, Zhang Z, Hu X, Zhang Y, Liu Y, Zhao Z, et al. ZnO nanoparticles induce apoptosis in HeLa cells. *J Pharm Pharmacol.* 2021;73(2):221–32.
70. Wu H, Zhang J. Chitosan-based zinc oxide nanoparticles for cervical cancer. *Saudi Pharm J.* 2018;26(2):205–10.
71. Muthulakshmi R, Rajeshkumar S, Manikandan V, Annadurai G, Manoharan C, Thirugnanasambandam R. Anticancer potential of ZnO nanoparticles synthesized using *Gracilaria edulis*. *Mater Sci Eng C Mater Biol Appl.* 2019;103:109840.
72. Yang Y, Ma Y, Liu Y, Chen L, Li X, Huang Q, et al. ZnO quantum dots induce oxidative stress and apoptosis. *Front Pharmacol.* 2020;11:131.
73. Moyo AA, Nkosi SS, Mhlanga SD, Mthunzi-Kufa P, Moloto MJ, Moloto N. Enhanced anticancer properties of biosynthesized zinc oxide. *J Mol Struct.* 2025;1328:141344.
74. Rahimi Kalateh Shah Mohammad G, Saboury AA, Falahati M, Mahdih Z, Gharavi S, Zare K, et al. Green synthesis of zinc oxide nanoparticles and biological properties. *J Biosci.* 2019;44(2):30.
75. Anjum S, Hashim M, Malik SA, Khan M, Lorenzo JM, Abbasi BH, et al. Recent advances in zinc oxide nanoparticles for cancer applications. *Cancers (Basel).* 2021;13(18).